# Characterization of NS 2028 as a specific inhibitor of soluble guanylyl cyclase

[1]Søren-Peter Olesen, Jørgen Drejer, Oskar Axelsson, Peter Moldt, *Lone Bang, *Jens Erik Nielsen-Kudsk, †Rudi Busse & †Alexander Mülsch

NeuroSearch, 26B Smedland, DK-2600 Glostrup, Denmark, *Department of Medicine B, Rigshospitalet, 2100 Copenhagen Ø, Denmark and †Zentrum der Physiologie, Klinikum der Johann Wolfgang Goethe-Universität, Theodor-Stern-Kai 7, 60590 Frankfurt a.M., Germany

**1** The haeme-containing soluble guanylyl cyclase ($\alpha_1\beta_1$-heterodimer) is a major intracellular receptor and effector for nitric oxide (NO) and carbon monoxide (CO) and mediates many of their biological actions by increasing cyclic GMP. We have synthesized new oxadiazolo-benz-oxazins and have assessed their inhibitory actions on guanylyl cyclase activity *in vitro*, on the formation of cyclic GMP in cultured cells and on the NO-dependent relaxation of vascular and non-vascular smooth muscle.

**2** Soluble guanylyl cyclase, purified to homogeneity from bovine lung, was inhibited by 4*H*-8-bromo-1,2,4-oxadiazolo(3,4-d)benz(b)(1,4)oxazin-1-one (NS 2028) in a concentration-dependent and irreversible manner ($IC_{50}$ 30 nM for basal and 200 nM for NO-stimulated enzyme activity). Evaluation of the inhibition kinetics according to Kitz & Wilson yielded a value of 8 nM for $K_i$, the equilibrium constant describing the initial reversible reaction between inhibitor and enzyme, and 0.2 min$^{-1}$ for the rate constant $k3$ of the subsequent irreversible inhibition. Inhibition was accompanied by a shift in the soret absorption maximum of the enzyme's haem cofactor from 430 to 390 nm.

**3** S-nitroso-glutathione-enhanced soluble guanylyl cyclase activity in homogenates of mouse cerebellum was inhibited by NS 2028 ($IC_{50}$ 17 nM) and by 17 structural analogues in a similar manner, albeit with different potency, depending on the type of substitution at positions 1, 7 and 8 of the benzoxazin structure. Small electronegative ligands such as Br and Cl at position 7 or 8 increased and substitution of the oxygen at position 1 by -S-,- NH- or -CH₂- decreased the inhibition.

**4** In tissue slices prepared from mouse cerebellum, neuronal NO synthase-dependent activation of soluble guanylyl cyclase by the glutamate receptor agonist N-methyl-D-aspartate was inhibited by NS 2028 ($IC_{50}$ 20 nM) and by two of its analogues. Similarly, 3-morpholino-sydnonimine (SIN-1)-elicited formation of cyclic GMP in human cultured umbilical vein endothelial cells was inhibited by NS 2028 ($IC_{50}$ 30 nM).

**5** In prostaglandin $F_{2\alpha}$-constricted, endothelium-intact porcine coronary arteries NS 2028 elicited a concentration-dependent increase (65%) in contractile tone ($EC_{50}$ 170 nM), which was abolished by removal of the endothelium. NS 2028 (1 $\mu$M) suppressed the relaxant response to nitroglycerin from 88.3 ± 2.1 to 26.8 ± 6.4% and induced a 9 fold rightward shift ($EC_{50}$ 15 $\mu$M) of the concentration-relaxation response curve to nitroglycerin. It abolished the relaxation to sodium nitroprusside (1 $\mu$M), but did not affect the vasorelaxation to the $K_{ATP}$ channel opener cromakalim. Approximately 50% of the relaxant response to sodium nitroprusside was recovered after 2 h washout of NS 2028.

**6** In phenylephrine-preconstricted, endothelium-denuded aorta of the rabbit NS 2028 (1 $\mu$M) did not affect relaxant responses to atrial natriuretic factor, an activator of particulate guanylyl cyclase, or forskolin, an activator of adenylyl cyclase.

**7** NO-dependent relaxant responses in non-vascular smooth muscle were also inhibited by NS 2028. The nitroglycerin-induced relaxation of guinea-pig trachea preconstricted by histamine was fully inhibited by NS 2028 (1 $\mu$M), whereas the relaxations to terbutaline, theophylline and vasoactive intestinal polypeptide (VIP) were not affected. The relaxant responses to electrical field stimulation of non-adrenergic, non-cholinergic nerves in the same tissue were attenuated by 50% in the presence of NS 2028 (1 $\mu$M).

**8** NS 2028 and its analogues, one of which is the previously characterized 1*H*-[1,2,4]oxadiazolo[4,3,-a]quinoxalin-1-one (ODQ), appear to be potent and specific inhibitors of soluble guanylyl cyclase present in various cell types. Oxidation and/or a change in the coordination of the haeme-iron of guanylyl cyclase is a likely inhibitory mechanism.

**Keywords:** Soluble guanylyl cyclase; cyclic GMP; cerebellum; endothelial cells; rabbit aorta; porcine coronary artery; guinea-pig trachea; nitric oxide; NS 2028 (4*H*-8-bromo-1,2,4-oxadiazolo(3,4-d)benz(b)(1,4)oxazin-1-one); ODQ (1*H*-[1,2,4]oxadiazolo[4,3,-a]quinoxalin-1-one)

## Introduction

Soluble guanylyl cyclases (sGC; GTP pyrophosphate-lyase (cyclizing)) comprise a family of heterodimeric haemoproteins which function biologically as intracellular nitric oxide (NO)

and, possibly, carbon monoxide (CO) receptors and effectors (Schmidt *et al.*, 1993). Guanosine 3′:5′-cyclic monophosphate (cyclic GMP) generated by guanylyl cyclases mediates several biological responses, such as vasodilatation, inhibition of platelet aggregation and neuronal signalling (Lincoln & Cornwell, 1993). A number of inhibitors of sGC have

[1] Author for correspondence.

previously been described, such as the redox-sensitive dyes methylene blue (Mayer *et al.*, 1993) and LY 83583 (Mülsch *et al.*, 1988), which inhibit sGC by both direct (Brüne *et al.*, 1990; Mülsch *et al.*, 1997) and indirect mechanisms (Gryglewski *et al.*, 1986), via generation of superoxide anion radicals. Additional, although more unspecific inhibitors of sGC include sulphydryl-blocking agents, such as disulphides (Brandwein *et al.*, 1981), o-iodosobenzoic acid (Ohlstein *et al.*, 1982), cytochrome P450 inhibitors such as SKF 525 (Förstermann *et al.*, 1988), and porphyrine derivatives (Ignarro *et al.*, 1984) including haeme (Ohlstein *et al.*, 1982). However, since some of these compounds also inhibit the membrane-bound particulate GC (O'Donnel & Owen, 1986; Ng & Diamond, 1986), NO synthases (Mülsch & Busse, 1990; Mayer *et al.*, 1993) and other enzymes (Luond *et al.*, 1993), and since superoxide and its metabolite hydrogen peroxide exhibit intrinsic biological activity the above-mentioned compounds are of limited value in studying the function of sGC in intact cells and organs.

In order to develop more specific inhibitors of sGC we synthesized a number of oxadiazolo-benz-oxazins (structure shown in Table 2) and tested their influence on the NO-stimulated activity of purified sGC, on NO-enhanced formation of cyclic GMP in neuronal tissue, vascular and non-vascular smooth muscle, and on endothelium-independent vasorelaxation. While this work was in progress one of the compounds under study (1*H*-[1,2,4]oxadiazolo[4,3-a]quinoxalin-1-one; ODQ) was independently described by others as a specific inhibitor of sGC (Garthwaite *et al.*, 1995). In the present study we extend these findings by showing that derivatives of the core structure exhibit even higher inhibitory potency against sGC. One derivative, NS 2028, was chosen for extensive analysis of its inhibitory action.

## Methods

### Assessment of guanylyl cyclase activity

*Soluble guanylyl cyclase from bovine lung*    The enzyme was purified to apparent homogeneity from bovine lung as described previously (Mülsch & Gerzer, 1991) and sGC activity was assessed by formation of cyclic [$^{32}$P]-GMP (Mülsch *et al.*, 1997). Briefly, sGC was incubated at 37°C for 10 min, unless indicated otherwise, in a triethanolamine-HCl-buffered solution (30 mM, pH 7.4), containing 100 $\mu$M [$\alpha$-$^{32}$P]-GTP (0.2 $\mu$Ci), 100 $\mu$M unlabelled cyclic GMP, 3 mM MgCl$_2$, 100 $\mu$g ml$^{-1}$ $\gamma$-globulin, 5 mM creatine phosphate, 100 $\mu$g ml$^{-1}$ creatine phosphokinase (1 unit ml$^{-1}$), 0.1 mM EGTA and 3 mM glutathione (GSH) (buffer I: final volume 100 $\mu$l). 3-Morpholino-sydnonimine (SIN-1) and NS 2028 were added as indicated in the Results section.

In dilution experiments designed to assess the reversibility of NS 2028-elicited inhibition, sGC was pre-incubated in the absence and presence of 300 nM NS 2028 in modified buffer I (containing unlabelled GTP), for 10 min at 37°C. Then the incubates were diluted 10 fold and sGC activity was assessed after addition of [$\alpha$-$^{32}$P]-GTP over a further 10 min incubation period in the presence of SIN-1 (100 $\mu$M) and either 300 or 30 nM NS 2028.

For evaluation of the inhibition kinetics according to Kitz & Wilson (1962), sGC was preincubated for 0, 3, 6 and 12 min at 37°C in modified buffer I as described above, with different concentrations of NS 2028 (0, 3, 10 and 30 nM). Then [$\alpha$-$^{32}$P]-GTP (10 $\mu$l) was added to an aliquot (90 $\mu$l) of the preincubate and formation of cyclic [$^{32}$P]-GMP

proceeded for 3 min at 37°C. The reaction was stopped by complexation of GTP with 450 $\mu$l zinc acetate (120 mM in water) and co-precipitation of Zn-GTP with zinc carbonate by addition of sodium carbonate (120 mM). The precipitate containing most of the [$\alpha$-$^{32}$P]-GTP was removed by centrifugation (10 min, 10,000 $\times$ g). The supernatant (900 $\mu$l) containing most of the cyclic [$^{32}$P]-GMP formed was mixed with 2 ml perchloric acid (0.1 M) and loaded ontop of a column (0.5 $\times$ 2 cm) bearing acid-activated (10 ml perchloric acid) alumina (alumina N, activity grade I; ICN Biomedicals, Eschwege, Germany). The column was washed twice with 10 ml water to remove residual [$\alpha$-$^{32}$P]-GTP and cyclic [$^{32}$P]-GMP was eluted directly into a scintillation vial by 5 ml Tris-HCl (0.5 M, pH 8). $^{32}$P was determined by liquid scintillation counting (Packard Tricarb 1900 TR). The recovery of cyclic GMP by this isolation procedure is 50 $\pm$ 3%, as determined independently by spiking the reaction mixtures with cyclic [$^3$H]-GMP and simultaneous counting of $^3$H and $^{32}$P in the column eluates after addition of 15 ml scintillation cocktail (Rotiszint eco plus; Carl Roth, Karlsruhe, Germany) and with appropriate settings of the $\beta$-counter energy windows.

The specific activity of sGC was calculated from the amount of cyclic [$^{32}$P]-GMP formed (nmol cyclic GMP mg$^{-1}$ GC min$^{-1}$). Determinations of sGC-activity were performed in duplicate and were repeated at least 3 times.

*Cerebellar soluble guanylyl cyclase*    Mouse cerebella were homogenized in a potter in 50 mM Tris-HCl at pH 7.6 and the homogenate was centrifuged at 18,000 r.p.m. (20,000 $\times$ g) for 50 min. Samples (100 $\mu$g protein) of the supernatant were added to a reaction mixture containing: 50 mM Tris-HCl (pH 7.6), 1.5 mM 1-methyl-3-isobutylxanthine (IBMX), 1 mM theophylline, 5 mM MnCl$_2$, 3 mM creatine phosphate, 94 $\mu$g ml$^{-1}$ creatine kinase, 94 $\mu$g ml$^{-1}$ bovine serum albumin, 30 $\mu$M GSNO, 300 $\mu$M GTP and NS 2028 or a derivative thereof at variable concentrations. The samples (0.5 ml final volume) were incubated for 10 min at 37°C, and the reaction was terminated by adding 10 $\mu$l 0.2 M EDTA followed by boiling for 3 min. The samples were centrifuged for 5 min at 14,000 r.p.m. and cyclic GMP and protein were determined in the resulting supernatant and the pellet, respectively.

*Cerebellar slices*    Cerebellae from 8–9 day old mice were sliced (400 $\mu$m thick) and incubated in Krebs-Henseleit buffer containing (in mM): NaCl 115, KCl 4.7, KH$_2$PO$_4$ 1.2, NaHCO$_3$ 25, MgSO$_4$ 1.2, CaCl$_2$ 2.5 and glucose 11. The slices were pretreated with NS 2028 for 7 min before they were challenged with either the glutamate-receptor agonist N-methyl-D-aspartate (NMDA) or the NO-donor S-nitrosoglutathione (GSNO) for 10 min. The reaction was terminated by filtration of the suspension and rapid submersion into boiling Tris-HCl (50 mM) at pH 7.6. The samples were homogenized on a potter and centrifuged at 14,000 r.p.m. for 5 min. The supernatant was taken for determination of cyclic GMP with a commercial $^3$H-radioimmunoassay kit (Amersham, U.K.) and the pellet used for protein determination. The cyclic GMP formation in each sample was calculated as pmol mg$^{-1}$ protein.

*Cultured cerebellar granule cells*    Neurones were isolated from 8–9 day old mice cerebella and plated in Petri dishes. The cerebellar granule cells constituted more than 90% of the population and they were maintained *in vitro* as described previously (Drejer *et al.*, 1983).

*Human cultured umbilical vein endothelial cells (HUVEC)*
Endothelial cells were isolated from human umbilical veins and
seeded in culture dishes (24-well, Falcon) as previously
described (Busse & Lamontagne, 1991). The cells were grown
in M199 medium and 20% heat-inactivated FCS (Vitromex)
supplemented with penicillin (50 u ml$^{-1}$), streptomycin
(50 $\mu$g ml$^{-1}$), L-glutamine (1 mM), glutathione (5 mg ml$^{-1}$),
and L(+)-ascorbic acid (5 mg ml$^{-1}$). Confluent cells were
washed with HEPES-modified Tyrode solution (15 mM
HEPES instead of 11 mM NaHCO$_3$; pH 7.4) and assessed for
formation of cyclic GMP elicited by SIN-1 (10 $\mu$M; 10 min)
after blockade of endothelial NO synthase by N$^G$-nitro-L-
arginine (L-NOARG; 30 $\mu$M, 30 min) and cyclic nucleotide
phosphodiesterase by isobutyl methyl xanthine (IBMX;
0.5 mM; 20 min). NS 2028 (30 and 300 nM) or its solvent was
added 5 min before SIN-1. The incubations were stopped by
removal of the cell supernatant (500 $\mu$l) and addition of ice-
cold trichloroactic acid (TCA; 600 $\mu$l; 6%). Cyclic GMP was
extracted from the TCA solution, acetylated and determined
by a commercially available radioimmunoassay kit. The
content of cyclic GMP was calculated as pmol per well, which
contained approximately 10$^5$ cells (30 $\mu$g protein).

## Assessment of relaxant responses

*Vascular smooth muscle*   Endothelium-intact vascular rings
were prepared from the distal part of the porcine left
anterior descending coronary artery (length 1.5 mm).
Endothelium-denuded rings were prepared from rabbit (male
New Zealand White; 2 kg) aorta (3 mm). The endothelium
was removed by gentle rubbing with a forceps. Each vessel
segment was mounted in a precision myograph for recording
of isometric tension changes (Nielsen-Kudsk *et al.*, 1986)
and suspended in Krebs solution (composition in mM: NaCl
118.0, KCl 4.6, CaCl$_2$ 2.5, MgSO$_4$ 1.15, NaHCO$_3$ 24.9,
KH$_2$PO$_4$ 1.15 and glucose 5.5) and gassed with a mixture of
95% O$_2$ and 5% CO$_2$ (pH 7.4; 37$^\circ$C). At the outset of each
experiment the coronary rings were stretched to a resting
tension of 2 g and the aortic rings to 3 g, to optimize
vasoconstrictor responses. Thereafter the rings were exposed
to K$^+$ (80 mM) as a test of vascular contractility. This
maximal contraction was taken as 100%. After washout
coronary rings were preconstricted by prostaglandin F$_{2\alpha}$
(PGF$_{2\alpha}$, 10 $\mu$M). When a stable contraction was established,
NS 2028 (0.1 – 1 $\mu$M) was added in a cumulative manner. In
another series of experiments concentration-relaxation curves
for nitroglycerin (NTG) and cromakalim, an opener of
ATP-sensitive K$^+$ channels (K$_{ATP}$), were obtained in the
presence and absence of NS 2028 (1 $\mu$M; 15 min preincuba-
tion).

In a further set of experiments conducted in the absence and
presence of NS 2028 (1 $\mu$M), phenylephrine (100 nM)-con-
stricted rabbit aortic rings were exposed to increasing
concentrations of either atrial natriuretic factor (ANF), an
activator of particulate GC, or forskolin. Indomethacin (3 $\mu$M;
coronary rings) or diclofenac (1 $\mu$M, rabbit aorta) was present
throughout the experiments to avoid interference from
prostanoids.

*Airway smooth muscle*   Tubular segments of trachea from
albino guinea-pigs (260 – 310 g), each comprising two
adjoining cartilage rings, were placed in the isometric
myographs under an initial resting tension of 0.6 g.
Following a 60 min equilibration period the preparations
were tested by K$^+$ (80 mM) depolarization and then
precontracted by histamine (2 $\mu$M). Concentration-relaxation

curves for nitroglycerin (NTG; 0.1 – 100 $\mu$M), vasoactive
intestinal peptide (VIP; 0.001 – 1 $\mu$M), terbutaline (0.003 –
10 $\mu$M) and theophylline (30 – 1000 $\mu$M) were obtained in the
absence and presence of NS 2028 (1 $\mu$M; 15 min preincuba-
tion).

To evaluate the possible involvement of the NO/cyclic
GMP pathway in inhibitory non-adrenergic non-cholinergic (i-
NANC) neurotransmission in the airways, tracheal rings
precontracted by histamine (2 $\mu$M) were subjected to four
repeated i-NANC stimulations at intervals of 20 min. NS 2028
(1 $\mu$M) was added after the first two i-NANC-induced
relaxations. A time-matched control tissue, which did not
receive NS 2028, was studied in parallel. i-NANC responses
were elicited by electrical field stimulation in the presence of
atropine (1 $\mu$M) and propranolol (1 $\mu$M) by use of an electrical
stimulator (Master 8, AMPI, Israel). Pulses of a supramaximal
strength (40 V, 10 Hz, 2 ms) were delivered in trains of 20 s
duration. The i-NANC relaxant responses were completely
blocked by tetrodotoxin (TTX) confirming that they were due
to nerve stimulation. Indomethacin (3 $\mu$M) was present
throughout all experiments to block endogenous formation of
cyclo-oxygenase products.

## Difference spectroscopy

A buffered solution (25 mM HEPES pH 7.4, 35 mM glycine,
5 mM Tris base, 10 mM 2-mercaptoethanol, 25% glycerol,
3% DMSO) of haeme-containing sGC (0.15 mg ml$^{-1}$,
haeme-content 0.2 mol haeme mol$^{-1}$ protein) was placed in
two microcuvettes (flow-through type, sample compartment
with 1 mm inner diameter, Hellma, Mülheim) and the
baseline difference spectrum from 580 to 380 nm was
recorded between both cuvettes in a double-beam spectro-
photometer (Kontron Uvikon 940 plus) at room tempera-
ture. Then 1 $\mu$l of a NS 2028 stock solution (300 $\mu$M in
DMSO) was mixed with the sGC in one cuvette (final
concentration of NS2028 10 $\mu$M) and 1 $\mu$l DMSO was added
to the other. After 10 min the difference spectrum was
recorded a second time. To reveal NS 2028-induced changes
the baseline difference spectrum was electronically subtracted
from the second spectrum.

To assess acid-induced changes in the Soret absorption the
difference spectrum between neutral and acidified (33 mM HCl,
final pH 2.0) sGC (1.5 mg ml$^{-1}$, 0.15 mol haeme mol$^{-1}$
protein) dissolved in buffer (20 mM triethanolamine hydro-
chloride, pH 7.4, 60% glycerol) was recorded at $-5^\circ$C.

## Data analysis

*Cyclic GMP formation in cerebellar tissue*   The NMDA- or
GSNO-stimulated cyclic GMP formation in the absence of NS
2028 was taken as 100% in each experimental series, and the
responses in the presence of NS 2028 were normalized relative
to this control value. Mean values $\pm$ s.e.mean are shown and
each point represents at least 6 experiments.

*Organ bath studies*   Relaxant responses are expressed as %
relaxation relative to the level of precontraction. EC$_{50}$ and E$_{max}$
values were estimated by fitting the concentration-relaxation
curves to the 3-parameter logistic equation (Hill-equation) by
use of non-linear regression analysis. Statistical significance
($P < 0.05$) was assessed by a two-way, unpaired Student's *t* test.

*Evaluation of irreversible inhibition kinetics*   GC inhibition
kinetics were assessed according to Kitz & Wilson (1962),
based on the following reaction scheme:

$$k3 \qquad k4$$
$$I + E \longleftrightarrow E \oplus I \longrightarrow E^* \longrightarrow E + I$$
$$K_i$$
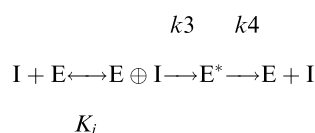
Assuming a small rate constant $k3$ for transformation of the reversible enzyme-inhibitor complex (E⊕I) into the irreversibly inhibited enzyme (E*), enzyme (E) and inhibitor (I) are in equilibrium ($K_i$) with E⊕I. In the case of irreversible inhibition $k4$ can be neglected. According to the integrated rate law derived from mass balances a plot of $1/k_{app}$ vs $1/(I)$ yields $k3$ and $K_i$:

$$\frac{1}{k_{app}} = \frac{1}{k3} + \frac{K_i}{k3} \bullet \frac{1}{[I]}$$

*Materials*

NS 2028, (4*H*-8-bromo-1,2,4-oxadiazolo(3,4-d)benz (b)(1,4) oxazin-1-one), all analogues of the compound, and GSNO (S-nitroso-glutathione) were synthesized at NeuroSearch. NMDA, IBMX, theophylline, creatine phosphate, creatine kinase, VIP, histamine, atropine, propranolol, terbutaline, atrial natriuretic factor (ANF), phenylephrine (PE), U 46619 (9,11-dideoxy-9α,11α-epoxymethanoprostaglandin $F_{2\alpha}$) and forskolin were obtained from Sigma (U.S.A.). Cromakalim was from Smith Kline Beecham (U.K.), nitroglycerin from DAK (Denmark), $PGF_{2\alpha}$ was from Pharmacia Upjohn (Belgium). SIN-1 was a generous gift from Cassella (Frankfurt). [α-$^{32}$P]-GTP and cyclic [$^3$H]-GMP was provided by NEN-Dupont (Dreieich, Germany).

## Results

*Actions of NS 2028 and analogues on sGC activity* in vitro

*Inhibition by NS 2028 of bovine lung soluble guanylyl cyclase* To assess the influence of NS 2028 (for structure see Table 2, compound 3) on cyclic GMP formation by sGC, the basal and NO-stimulated enzyme activity was measured during a 10 min incubation in the absence and presence of 3-morpholino-sydnonimine (SIN-1; 100 $\mu$M), an NO-donor (Bohn & Schonafinger, 1989), and various concentrations of NS 2028. NS 2028 inhibited both the basal and SIN-1-stimulated GC activity (Figure 1a,b) in a concentration-dependent manner. In the presence of 100 $\mu$M GTP, NS 2028

inhibited the SIN-1-stimulated GC activity less potently (IC$_{50}$ = 200 n$_M$) than the basal GC activity (IC$_{50}$ = 30 n$_M$). During a 10 min incubation complete inhibition of basal activity could not be attained.

In order to evaluate the influence of NS 2028 on the affinity of sGC for its substrate, the enzyme activity was also measured in the presence of two lower concentrations of GTP (10 and 30 $\mu$M). As shown in Figure 1 the concentration of NS 2028 required for half-maximal inhibition of either the basal or SIN-1-stimulated GC activity was not affected by the GTP concentration. Evaluation of the enzyme kinetics by classical Michealis-Menton plots revealed that the $K_m^{GTP}$ was unchanged (basal: 50 ± 4 $\mu$M, with 300 n$_M$ NS 2028: 40 ± 3 $\mu$M; SIN-1: 20 ± 3 $\mu$M, with NS 2028: 22 ± 4 $\mu$M). Thus, NS 2028 appears to inhibit sGC by decreasing the maximal catalytic rate ($V_{max}$).

*Reversibility and time-dependence of inhibition* To investigate the reversibility of the NS 2028-induced inhibition of sGC, the enzyme was preincubated with or without NS 2028 (300 n$_M$) for 10 min, then diluted 10 fold and assessed immediately for a further 10 min for basal and SIN-1-stimulated catalytic activity, in the absence and presence of either 30 or 300 n$_M$ NS 2028. The degree of inhibition of basal as well as SIN-1-enhanced activity was not reversed by dilution (Table 1). Rather the activity of the NS 2028-

**Table 1** Inhibition of basal and SIN-1-stimulated sGC activity by NS 2028 was not reversible by dilution
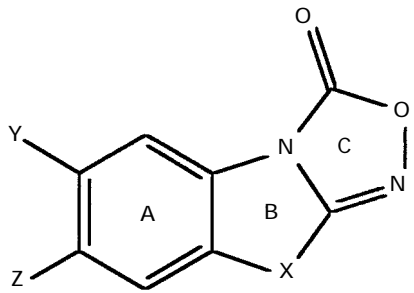
| Concentration of NS 2028 (n$_M$) | | sGC-activity (nmol mg$^{-1}$ min$^{-1}$) | |
| --- | --- | --- | --- |
| *Preincubation* | *Incubation* | *Basal* | *SIN-1-stimulated* |
| 0 | 0 | 9.6 ± 1.7 | 384 ± 10 |
| 0 | 30 | 6.2 ± 0.4 | 370 ± 12 |
| 0 | 300 | 2.4 ± 0.1 | 204 ± 8 |
| 300 | 30 | 1.2 ± 0.1 | 49 ± 1 |
| 300 | 300 | 1.3 ± 0.1 | 30 ± 2 |

Purified sGC was preincubated for 10 min (37°C) with or without NS 2028 (300 n$_M$), then diluted 10 fold and assessed for basal and SIN-1-stimulated activity in the absence and presence of 30 n$_M$ and 300 n$_M$ NS 2028. Data represent mean ± s.e.mean from 3 experiments performed in duplicate.
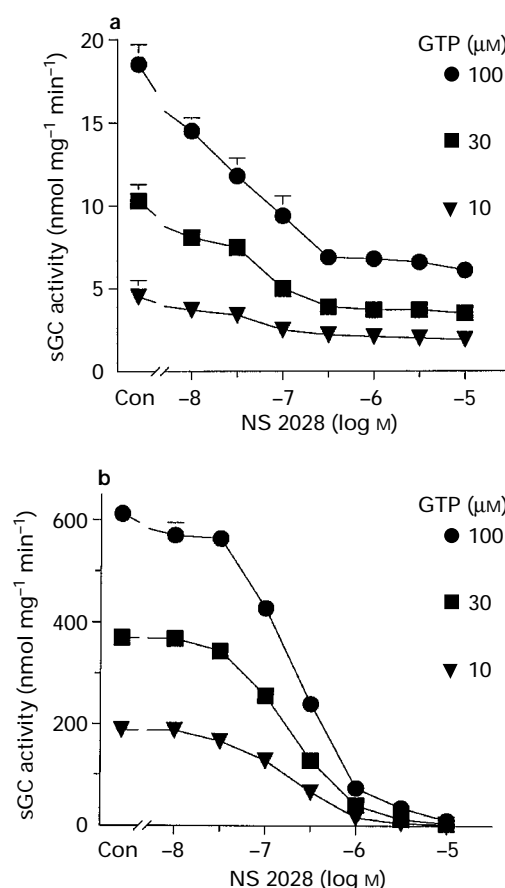


**Figure 1** Effect of the substrate (GTP) concentration on the NS 2028-induced inhibition of basal (a) and SIN-1-stimulated (b) activity of sGC from bovine lung. sGC activity was determined for 10 min (37°C) in the absence (a) and presence (b) of 100 $\mu$M SIN-1, with various concentrations of GTP (10, 30, 100 $\mu$M) and in the absence (Con) and presence of NS 2028 (10 n$_M$ – 10 $\mu$M, as indicated on the x-axis). The data represent the mean from 3 experiments performed in duplicate; vertical lines show s.e.mean when larger than symbols.

**Table 2** Inhibition of GSNO (30 $\mu$M)-stimulated soluble guanylyl cyclase from mouse cerebellum by analogues of NS 2028

| Compound no. | X | Y | Z | Guanylyl cyclase $IC_{50}$ ($\mu$M) |
|---|---|---|---|---|
| 1 | $OCH_2$ | H | H | 0.20 |
| 2 | $OCH_2$ | H | F | 0.08 |
| 3 (NS 2028) | $OCH_2$ | Br | H | 0.017 |
| 4 | $OCH_2$ | H | Br | 0.01 |
| 5 | $OCH_2$ | $NO_2$ | H | 0.05 |
| 6 | $OCH_2$ | OMe | H | 0.08 |
| 7 | $OCH_2$ | $CF_3$ | H | 0.04 |
| 8 | $OCH_2$ | Ph | H | 0.14 |
| 9 | $OCH_2$ | t-Bu | H | 0.04 |
| 10 | $OCH_2$ | H | t-Bu | 0.14 |
| 11 (ODQ) | NCH | H | H | 0.08 |
| 12 | NCH | H | $NO_2$ | 0.06 |
| 13 | NCH | Br | H | 0.01 |
| 14 | NCH | Cl | H | 0.01 |
| 15 | $SCH_2$ | H | H | 0.16 |
| 16 | $CH_2S$ | H | H | 0.30 |
| 17 | $HNCH_2$ | H | H | 4.1 |
| 18 | $CH_2CH_2$ | H | H | >3.0 |

The table correlates modifications of the chemical core structure (as indicated in the scheme) to the potency of the respective compound to inhibit sGC from mouse cerebellum. For details see text.

preincubated enzyme was inhibited by 30 or 300 nM NS 2028 to a much greater extent than the non-preincubated enzyme. This finding shows that sGC is irreversibly inhibited by NS 2028 and further suggests that the extent of this inhibition increases with time.

To investigate further the latter observation the time course of inhibition by NS 2028 of SIN-1(100 $\mu$M)-enhanced sGC activity was assessed by performing activity determinations of different duration (1, 3, 10, 20 and 30 min), either in the absence or presence of NS 2028 (300 nM). The SIN-1-elicited activation of sGC exhibited a biphasic time-course and maximal activation was achieved within 10 min of incubation (Figure 2a). The degree of inhibition by NS 2028 increased progressively with time, from no apparent inhibition recognizable after 1 min to approximately 70% inhibition after 30 min of incubation (Figure 2b).
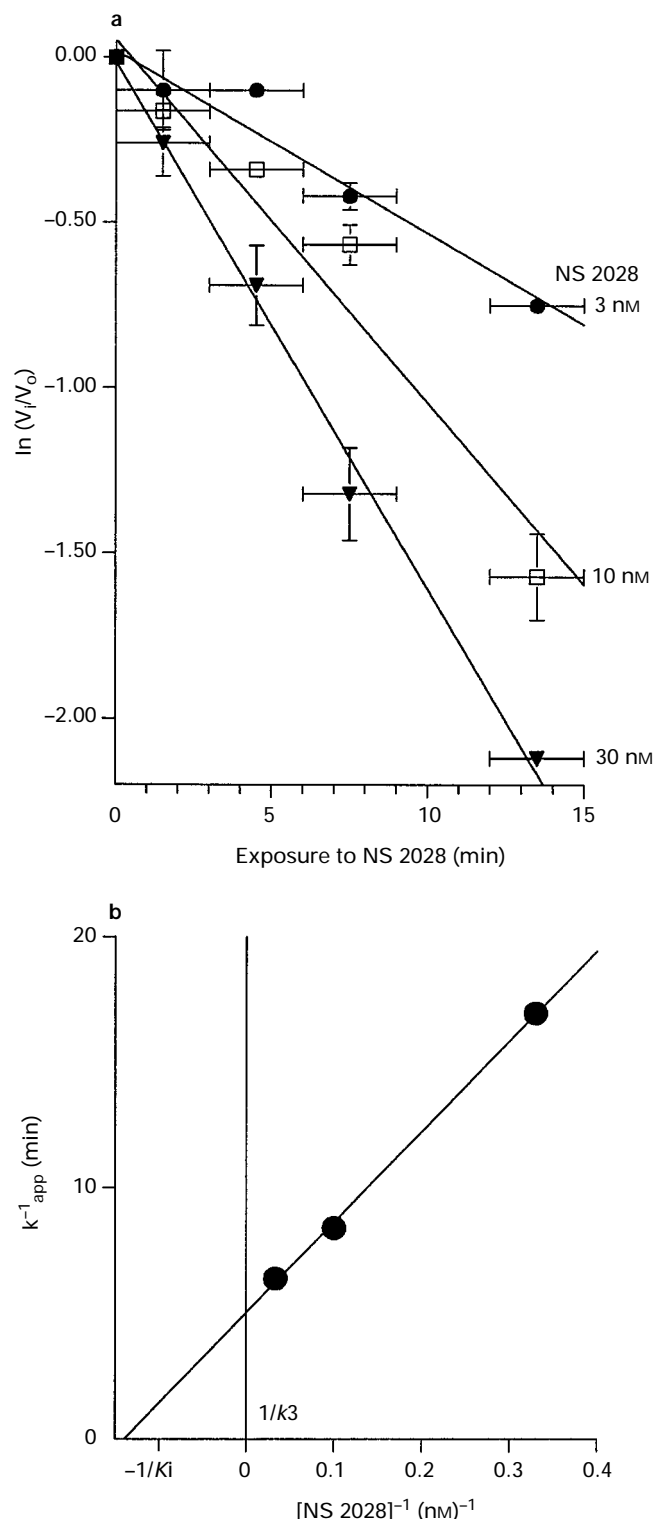
*Kinetics of irreversible inhibition*    In the experiments illustrated in Figure 2 the extent of inhibition during prolonged incubation (30 min) is an average over this incubation period and, therefore, does not correctly reflect the momentary extent of inhibition at a certain time. Therefore, in order to evaluate the true kinetics of irreversible inhibition sGC was preincubated with different concentrations of NS 2028 for the periods indicated in Figure 3a and then assessed for basal enzyme activity for 3 min. A semi-logarithmic plot of the fraction of non-inhibited enzyme activity (ln ($V_i/V_o$)) vs preincubation time
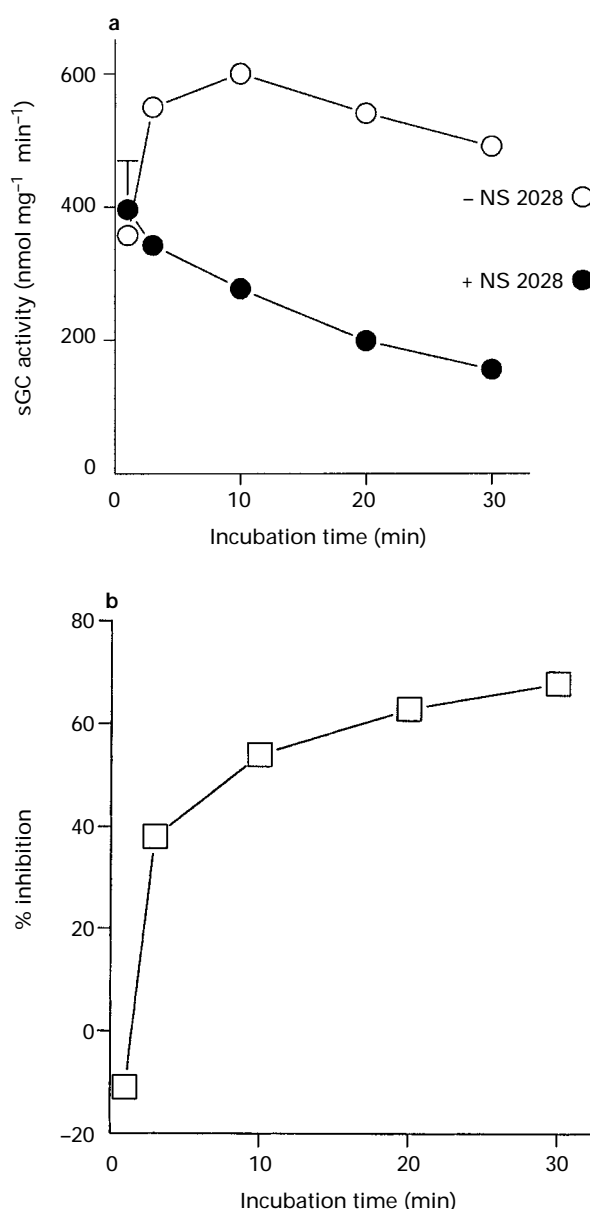


**Figure 2** Time course of inhibition of SIN-1-stimulated sGC-activity by NS 2028. (a) The activity of SIN-1 (100 $\mu$M)-stimulated sGC from bovine lung was assessed for 1, 3, 10, 20 and 30 min in the absence and presence of NS 2028 (300 nM). (b) The % inhibition was calculated for each time point. The data represent the mean from 3 experiments performed in duplicate; vertical lines show s.e.mean.

yielded linear graphs. The steepness of these graphs (equivalent to the apparent rate constant of irreversible inhibition $k_{app}$) increased with the concentration of inhibitor applied (Figure 3a). A double-reciprocal replot of $k_{app}$ vs concentration of NS 2028 (Kitz & Wilson, 1962) fitted to a linear relationship (Figure 3b) from which a value of 0.2 min$^{-1}$ was derived for $k3$, the truth rate constant of irreversible inhibition, and a value of 8 nM for $K_i$, the thermodynamic constant for the rapid pre-equilibrium between NS 2028 and sGC.

*NS 2028-induced changes in the absorbance spectrum of the haeme-cofactor of sGC*    A 10 min exposure of sGC to NS 2028 (10 $\mu$M) at 20°C induced characteristic changes in the absorbance spectrum of its haeme-cofactor. As shown in the difference spectrum recorded between NS 2028-exposed and non-exposed sGC (Figure 4), a large absorbance decrease at 435 nm was accompanied by increases at 390 nm and 470 to

**Figure 3** Evaluation of the kinetics of irreversible inhibition of sGC by NS 2028. sGC was pre-incubated with NS 2028 (3, 10, 30 nM) for the time periods indicated and was immediately assessed for basal catalytic activity over the subsequent 3 min. (a) Semilogarithmic plot of residual sGC-activity vs incubation time. Graphs represent best linear fits by regression analysis and their steepness is equivalent to the apparent rate constant $k_{app}$ of irreversible inhibition. Data (mean ± s.e.mean) from three experiments performed in duplicate. Vertical error bars represent s.e.mean of GC-activity determinations, horizontal bars indicate the time period during which GC-activity was determined. (b) Replot of $1/k_{app}$ derived from (a) vs $1/$ concentration of NS 2028. The x-axis intercept equals - $1/K_i$, the y-axis intercept $1/k3$. For explanation see text.

500 nm. A similar 'bleaching' of the haeme's Soret absorption was observed when sGC was treated with mild acid (pH 2) at subzero temperatures ($-5°C$; Figure 4) or by $K_3[Fe(CN)_6]$ (data not shown). According to the spectra shown the absorbance change ($\Delta E_{390} + \Delta E_{435}$) mol haeme was 75000 $M^{-1}$ $cm^{-1}$ for the NS 2028-inhibited vs non-inhibited sGC and 78000 $M^{-1}$ $cm^{-1}$ for the acidified vs neutral sGC. Acidified and $K_3[Fe(CN)_6]$-oxidized sGC is inactive and the acidified sGC remains inactive after neutralization (data not shown). These findings indicate that NS 2028 alters the oxidation state and/or coordination of the haeme-iron of sGC.

*Inhibitory potency of different NS 2028-analogues* A crude preparation of sGC from mouse cerebellum was used to screen different structural analogues of NS 2028 for their inhibitory potency. Stimulation of this enzyme by 30 $\mu$M S-nitrosoglutathione (GSNO) increased the GC activity from 261 to 9269 pmol cyclic GMP $mg^{-1}$ 10 $min^{-1}$ and this activation was inhibited in a concentration-dependent manner by NS 2028 ($IC_{50}$ 17 nM; Table 2, compound 3). As observed with the bovine purified lung enzyme, the $IC_{50}$ for inhibition of the mouse cerebellar sGC by NS 2028 was not affected by the substrate concentration within the range $30-1000$ $\mu$M GTP
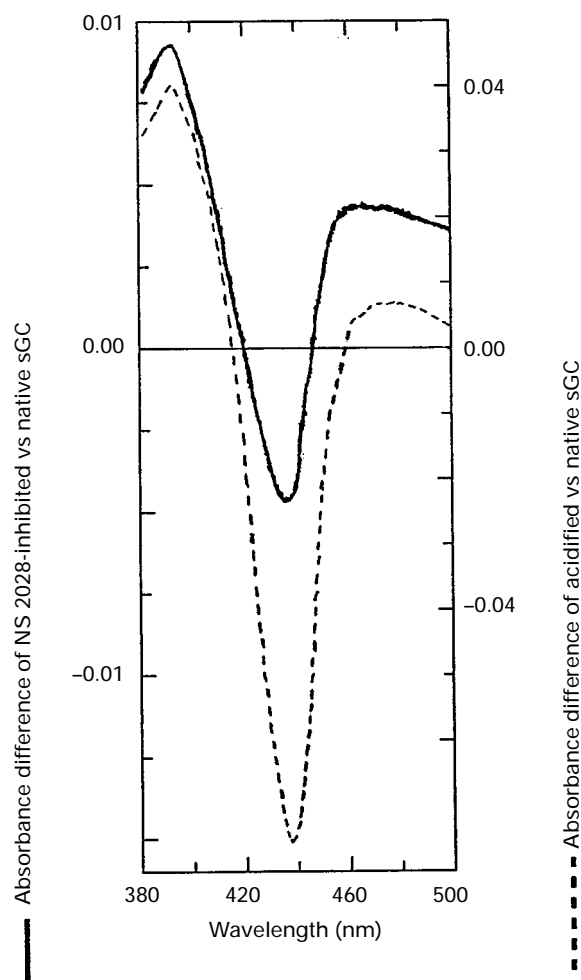


**Figure 4** Visible difference spectra of NS 2028-inhibited and acidified sGC. The difference spectrum of NS 2028 (10 $\mu$M; 10 min)-inhibited vs native haeme-containing sGC (0.2 $\mu$M in haeme) was recorded at room temperature in a double-beam spectrophotometer (left scale). The difference spectrum between neutral and acidified (33 mM HCl, final pH 2.0) sGC (1.5 $\mu$M in haeme) was recorded at $-5°C$ (right scale). The spectra are representative of three recorded with different sGC preparations.
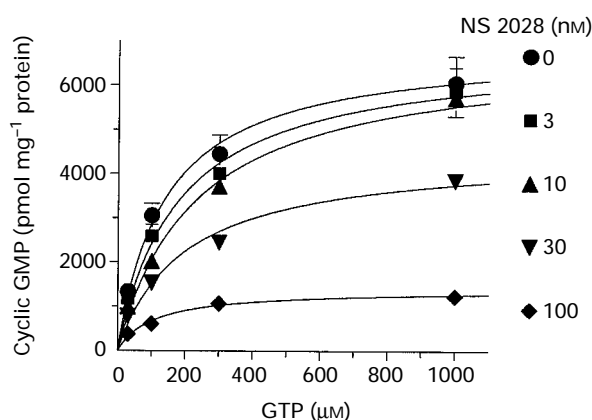
**Figure 5** Influence of the substrate (GTP) concentration on the NS 2028-induced inhibition of GSNO-stimulated activity of sGC from mouse cerebellum. The GSNO (30 $\mu$M)-stimulated activity of sGC in the $10000 \times g$ supernatant from mouse cerebellum homogenates was assessed in the presence of various concentrations of GTP and NS 2028 (0, 3, 10, 30, 100 nM). Cyclic GMP was detected by radioimmunoassay. The data were fitted to the simple Michaelis-Menten-relationship (line graphs). Mean values of 3 experiments performed in triplicate are shown; vertical lines indicate s.e.mean.

(Figure 5). Similarly, the decrease in sGC activity in this crude preparation could be attributed to a decrease in $V_{max}$, while $K_m^{GTP}$ remained unaffected. Seventeen structural analogues of NS 2028 all elicited a concentration-dependent inhibition of cerebellar sGC, the most potent being compounds 4, 13 and 14 with an $IC_{50}$ of 10 nM (Table 2), closely followed by compound 3, which is NS 2028. For comparison, ODQ (compound 11) was about 5 fold less potent than NS 2028.

## Effect of NS 2028 and its analogues in biological systems

*Cyclic GMP formation in neuronal tissue* In cerebellar slices, basal cyclic GMP formation was increased from 1.8 pmol mg$^{-1}$ protein to 19.7 pmol mg$^{-1}$ protein after 7 min incubation with the glutamate receptor agonist N-methyl-D-aspartate (NMDA). NMDA stimulates sGC indirectly via activation of neuronal NO synthase. NS 2028 inhibited this cyclic GMP formation in a concentration-dependent manner ($IC_{50}$ 19 nM; Figure 6a). The response to NMDA was completely inhibited by 300 nM NS 2028. Two analogues of NS 2028, NS 2014 (compound 13) and NS 2001 (compound 1), where approximately 2 fold and 15 fold less potent inhibitors than NS 2028 ($IC_{50}$ 35 and 250 nM, respectively; Figure 6a), in accordance with their potency at inhibiting the crude cerebellar sGC (Table 2).

*Cyclic GMP formation in cultured cerebellar granule cells* In cultured cerebellar granule cells a similar concentration-dependent inhibition by NS 2028 of the NMDA-induced cyclic GMP formation was observed, albeit with a higher $IC_{50}$ value of 60 nM (Figure 6b). Since NS 2028 had no significant affinity for glutamate-receptors, as assessed by [$^3$H]-glutamate ligand binding (no affinity at 10 $\mu$M; data not shown), the results suggest that the inhibition of cyclic GMP formation was due to a direct effect on the cerebellar GC.

*Cyclic GMP formation in human umbilical vein endothelial cells (HUVEC)* The basal level of cyclic GMP (73 fmol/well) in cells that had been pretreated for 20 min with the NO synthase inhibitor N$^G$-nitro-L-arginine (30 $\mu$M) was enhanced approximately 28 fold by 10 $\mu$M SIN-1. NS 2028 concentration-
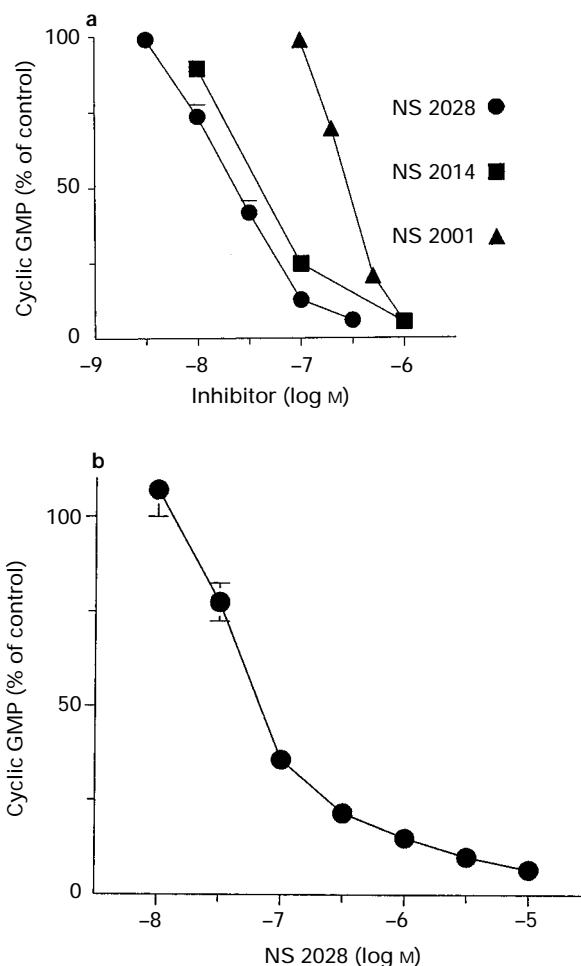


**Figure 6** Inhibition of cyclic GMP accumulation in mouse cerebellum. (a) Cerebellar slices: concentration-dependent inhibition of the NMDA (100 $\mu$M)-induced cyclic GMP formation by NS 2028, compound 1 (NS 2001) and compound 13 (NS 2014). Cyclic GMP was determined by radioimmunoassay. Each data point represents the mean value obtained with slices from 6 different animals. (b) Primary culture of cerebellar granule cells: concentration-dependent inhibition of the NMDA(100 $\mu$M)-induced cyclic GMP formation by NS 2028. Mean values of 4 independent experiments. In (a) and (b), vertical lines show s.e.mean.

dependently inhibited SIN-1-elicited cyclic GMP formation, half-maximally at 30 nM (Figure 7). 'Basal' levels of cyclic GMP were not affected by NS 2028 (300 nM) in these N$^G$-nitro-L-arginine-pretreated cells, presumably because they originated from the particulate GC.

*Contractility of vascular smooth muscle* When NS 2028 (0.1 – 1 $\mu$M) was added to porcine isolated coronary arteries preconstricted by PGF$_{2\alpha}$ it produced a supplementary concentration-dependent contraction ($EC_{50}$ 170 $\pm$ 4 nM; Figure 8a). This contraction depended on the presence of the endothelium (data not shown) and amounted to 65.2 $\pm$ 7.8% of maximal contractile responses to K$^+$ (80 mM). NTG (0.001 – 100 $\mu$M) relaxed the isolated coronary vessels half-maximally at 1.6 $\pm$ 0.2 $\mu$M and elicited a maximal relaxation of 88.3 $\pm$ 2.1% (Figure 9a). The vasorelaxant response to NTG was inhibited by NS 2028 (1 $\mu$M), which shifted the NTG concentration-relaxation curve to the right ($EC_{50}$ 14.8 $\pm$ 5.5 $\mu$M) and suppressed the maximal relaxation by NTG to 26.8 $\pm$ 6.4% (Figure 9a). In contrast, NS 2028 (1 $\mu$M) did not significantly influence the concentration-relaxation relationship

to cromakalim (0.1 – 100 $\mu$M; $EC_{50}$ 8.6 $\pm$ 3.0 in the absence and 16 $\pm$ 5 $\mu$M in the presence of NS 2028; data not shown).

To investigate the reversibility of the NS 2028-induced inhibition of sGC and NO-mediated relaxations of vascular segments, coronary artery rings constricted to 90 $\pm$ 4% of the KCl (80 mM)-induced tone by the $PGF_{2\alpha}$ derivative U-46619 (1 $\mu$M), were relaxed (53 $\pm$ 2.4%; $n=4$) by sodium nitroprusside (SNP; 1 $\mu$M). Fifteen minutes later two rings were exposed

to NS 2028 (1 $\mu$M) for 20 min to abolish the SNP-elicited relaxation. Thereafter the rings were thoroughly washed for 2 h by frequent changes of the bathing medium, until resting tone was achieved. Subsequently the rings were again constricted by U 46619 and relaxed by SNP. While the relaxant responses to the second SNP challenge were not affected in control rings (62.8 $\pm$ 2%), rings exposed to NS 2028 relaxed by only 28.5 $\pm$ 0.7%. This finding suggests that the NS 2028-induced inhibition of sGC in porcine coronary arteries is slowly reversible.

In order to exclude particulate GC and adenylate cyclase as potential biological targets of NS 2028 the relaxant responses of phenylephrine-constricted endothelium-denuded rabbit aortic rings to atrial natriuretic factor (ANF) and forskolin were assessed. Both agonists elicited concentration-dependent relaxations ($EC_{50}$ 2 $\pm$ 0.6 nM and 30 $\pm$ 4 nM, respectively). Preincubation (20 min) of rings with NS 2028 (1 $\mu$M) was without effect on these relaxant responses (data not shown).
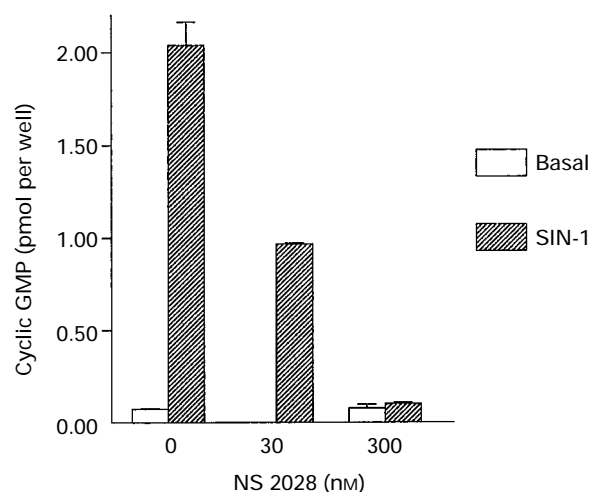


**Figure 7** Inhibition by NS 2028 of SIN-1-elicited formation of cyclic GMP in HUVEC. The effect of NS 2028 on the SIN-1-induced increase in cyclic GMP was assessed in human cultured umbilical vein endothelial cells (HUVEC) in the presence of $N^G$-nitro-L-arginine (30 $\mu$M) and IBMX (0.5 mM). HUVEC were incubated for 15 min with or without NS 2028 in the absence (basal) and presence of SIN-1 (10 $\mu$M) during the final 10 min. Cyclic GMP was determined by radioimmunoassay. The data are mean values $\pm$ s.e.-mean from one experiment and are representative of data obtained in two additional experiments.
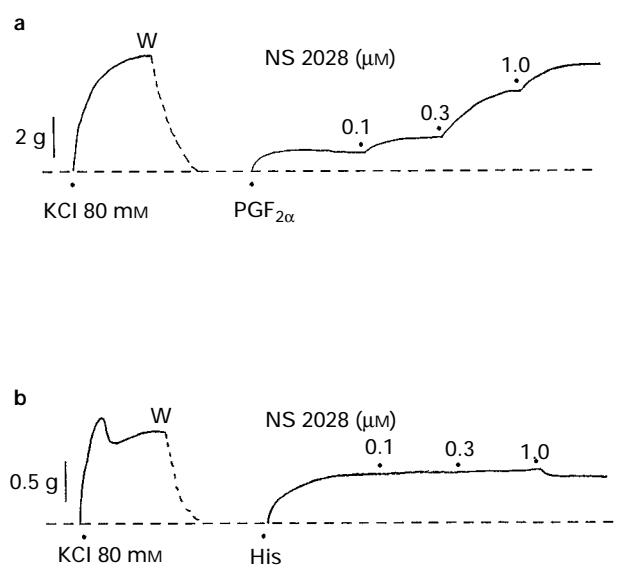


**Figure 8** Original recordings illustrating the effect of NS 2028 on (a) a porcine isolated coronary artery and (b) a guinea-pig trachea. After the contractile response to membrane depolarization ($K^+$ 80 mM) had been assessed the isolated rings were washed (W) and then constricted submaximally by either (a) $PGF_{2\alpha}$ (10 $\mu$M) or (b) histamine (His; 2 $\mu$M). Both smooth muscle preparations were then exposed to increasing concentrations of NS 2028 (0.1, 0.3, 1.0 $\mu$M). These tracings are representative of 6 separate experiments.
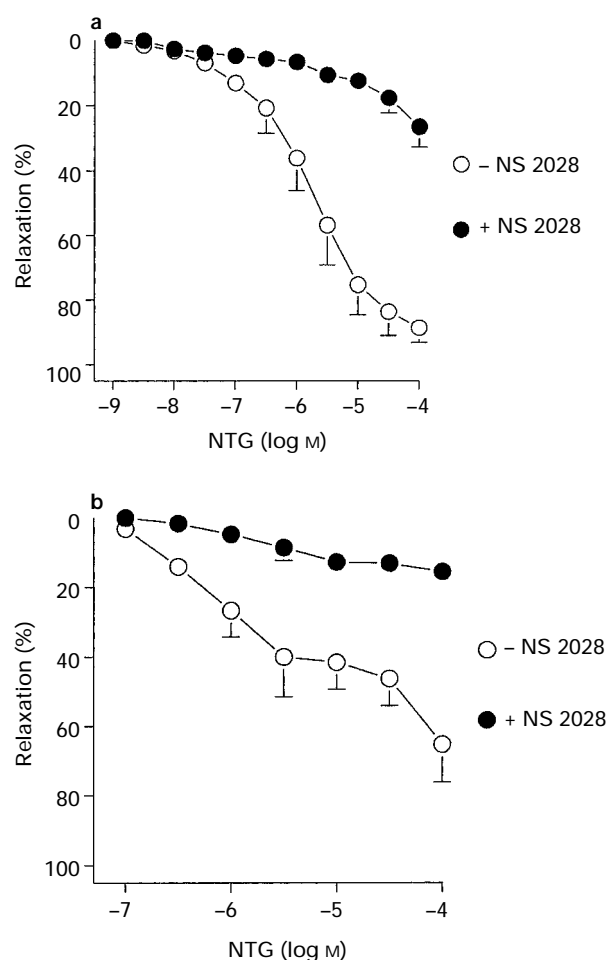




**Figure 9** Concentration-relaxation curves for nitroglycerin (NTG) in (a) porcine isolated coronary arteries and (b) guinea-pig trachea. (a) Isolated endothelium-intact coronary arteries of the pig were preconstricted with $PGF_{2\alpha}$ (10 $\mu$M) and then relaxed by increasing concentrations of NTG (1 nM – 100 $\mu$M). NS 2028 (1 $\mu$M) was either absent or added 15 min before the relaxant responses were assessed. The data represent mean values from 6 experiments. (b) Isolated rings of guinea-pig trachea were preconstricted by histamine (2 $\mu$M) and then relaxed by increasing concentrations of NTG (100 nM – 100 $\mu$M). NS 2028 (1 $\mu$M) was either absent or added 15 min before the relaxant responses were assessed. The data represent mean values from 6 experiments. In (a) and (b), vertical lines show s.e.mean.

*Airway smooth muscle*   NS 2028 (0.03–1 $\mu$M) did not induce any additional contraction when added to histamine-precontracted tracheal rings (Figure 8b). In contrast, NS 2028 (1 $\mu$M) had a small relaxant effect on airway smooth muscle. NTG (0.1–100 $\mu$M) relaxed the guinea-pig trachea by 84.1 $\pm$ 8.4% (EC$_{50}$ 25 $\pm$ 12 $\mu$M), an effect which was almost abolished by NS 2028 (1 $\mu$M) (Figure 9b). In contrast, concentration-relaxation response curves for VIP (0.001–1 $\mu$M; EC$_{50}$ 68 $\pm$ 15 vs 100 $\pm$ 20 nM; control vs NS 2028), terbutaline (0.003–10 $\mu$M; EC$_{50}$ 100 $\pm$ 12 vs 130 $\pm$ 18 nM) and theophylline (30–1000 $\mu$M; EC$_{50}$ 180 $\pm$ 20 vs 200 $\pm$ 25 $\mu$M) were not influenced by NS 2028 (1 $\mu$M). In histamine-precontracted trachea, electrical field stimulation in the presence of atropine, propranolol and indomethacin evoked i-NANC relaxant responses that were reproducible upon repeated stimulation (Figure 10). NS 2028 (1 $\mu$M) reduced the i-NANC responses from 53.1 $\pm$ 7.9 to 28.5 $\pm$ 6.0% relaxation.
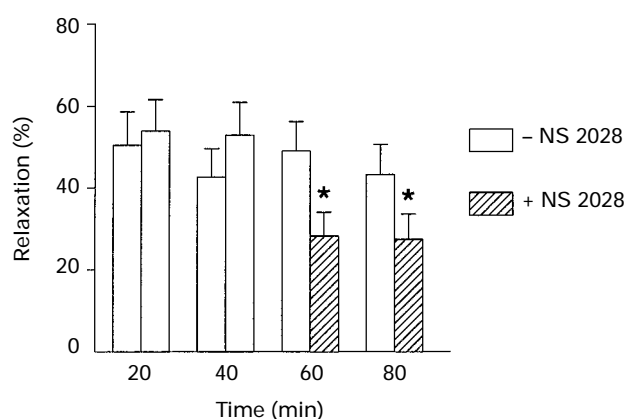
## Discussion

In the present study we observed a potent inhibition of basal and NO-stimulated activity of isolated sGC by NS 2028, which increased with time by monoexponential kinetics and was not reversible by dilution, similar to previous findings for the NS 2028-analogue ODQ (Schrammel *et al.*, 1996). Evaluation of the kinetics of irreversible inhibition yielded a rate constant $k3$ of 0.2 min$^{-1}$, which describes the conversion of the preformed reversible NS 2028/sGC complex into the irreversibly inhibited enzyme. The dissociation constant $K_i$ for formation of the reversible complex was 8 nM, which underlines the high affinity of NS 2028 for an as yet unidentified binding site on sGC. With regard to this binding site and the mechanism of inhibition, we observed a blueshift of the Soret maximum of the haeme-cofactor of sGC, indicating that the haeme could be a target site of NS 2028. The same spectral shift has previously been described with ODQ (compound 11) acting on a similar sGC preparation from bovine lung, which rendered the



**Figure 10** Effect of NS 2028 on inhibitory non-adrenergic, non-cholinergic (i-NANC) relaxant responses of guinea-pig trachea. The i-NANC responses were induced by electrical field stimulation (40 V, 10 Hz, 2 ms) in histamine (2 $\mu$M)-precontracted rings of guinea-pig trachea, in the presence of atropine and propranolol (both 1 $\mu$M). The mean i-NANC responses at each of four repeated stimulations of control tissues are represented by the lefthand columns at each time point, while those of the test tissues are represented by the righthand columns. Of these, the first two responses were recorded in the absence, and the 3$^{rd}$ and 4$^{th}$ response in the presence of NS 2028 (1 $\mu$M). *Indicates significantly different responses between control and NS 2028-treated rings ($P < 0.05$). Data represent mean values $\pm$ s.e.mean from 6 experiments.

enzyme unresponsive to NO (Schrammel *et al.*, 1996), and with K$_3$[Fe(CN)$_6$] (Stone *et al.*, 1996; and this study). In the latter case, formation of a high-spin ferric haeme was detected by e.s.r. spectroscopy (Stone *et al.*, 1996). Therefore, it is conceivable that NS 2028 and its derivatives alter the oxidation state and/or coordination of the haeme-iron of sGC. Since acidification of sGC at subzero temperatures (to avoid denaturation and precipitation of the protein) induced similar changes in the absorbance spectrum, and since this treatment mobilizes haeme from the enzyme protein (Gerzer *et al.*, 1982), it is furthermore likely that the absorbance changes associated with inhibition of sGC by NS 2028 could be explained by similar molecular mechanisms. The haeme-iron in native resting sGC is in the 5-coordinated ferrous high spin state (Stone & Marletta, 1995), one axial ligand is histidine 105 of the $\beta_1$ subunit (Wedel *et al.*, 1994). Access to the free axial position seems to be sterically and electrostatically hindered (Kim *et al.*, 1996), and only small molecules like NO, CO and nitrosomethan, but not O$_2$, have previously been shown to bind to the ferrous haeme-iron (Gerzer *et al.*, 1981; Mülsch & Böhme, 1984; Stone & Marletta, 1995). Therefore it is quite remarkable that comparatively large molecules like NS 2028 and ODQ should be able to interact with the haeme-iron of sGC. However, assuming that the rate constant of irreversible inhibition $k3$ reflects the rate of the irreversible changes induced by NS 2028 at the haeme, this low rate (0.2 min$^{-1}$) is in accordance with the hypothesis that NS 2028 interacts directly with the haeme. Interestingly, the analogous compound ODQ did not inhibit NO synthase (Garthwaite *et al.*, 1995), a ferric haeme-protein depending on oxygen-binding to its haeme for catalysis, supporting the notion that the interaction this class of sGC inhibitors with protein-bound haeme is influenced by the structure of the haeme-binding pocket, as well as the nature of axial ligands and the spin state of the haeme-iron.

The structure-activity relationship of the present series of compounds shows that there are very few modifications compatible with high inhibitory potency (Table 2). Substitution of position 7 or 8 in the A-ring by bromine or chlorine results in high inhibitory potency, whereas only substitution of oxygen by imino nitrogen, ether or thioether are acceptable in ring B. Ring expansion leads to loss of inhibitory activity, since it interrupts conjugation between rings A and C. The C-ring is the most crucial part of the molecule and no modifications have been found to be compatible with inhibitory activity (unpublished results). As illustrated by Table 2, the previously characterized ODQ (compound 11) is not the most potent of this class of inhibitors. NS 2028 and compounds 4, 13 and 14 were 5 to 8 fold more potent inhibitors of the cerebellar sGC. Our data on the inhibitory potency of ODQ on cerebellar sGC are consistent with those obtained by others in NMDA-stimulated cerebellar slices (Garthwaite *et al.*, 1995). However, NS 2028 and ODQ seem to be equally potent inhibitors of NO-stimulated sGC purified from bovine lung (Garthwaite *et al.*, 1995).

We observed that NS 2028 specifically inhibited NO-dependent cyclic GMP formation and cellular responses in a number of biological systems, whereas cromakalim-, ANF-, and forskolin-dependent vascular relaxations were not significantly affected, thus underlining the specificity of NS 2028 and its derivatives for inhibition of sGC-dependent processes. Inhibition of NO-stimulated sGC by NS 2028 and the various analogues due to a chemical inactivation of NO is very unlikely, since this has been experimentally excluded in case of ODQ (Garthwaite *et al.*, 1995). Further evidence in favour of a direct inhibition of the enzyme stems from our observation

that basal and $3'$-($5'$-hydroxymethyl-$2'$-furyl)-1-benzyl indazole (YC-1)-stimulated sGC activity was also inhibited by NS 2028 (Mülsch *et al.*, 1997). However, the influence of NS 2028 on NO release from NO donors has to be measured in the target tissues before additional effects of NS 2028 on the biotransformation of NO donors can definitely be excluded. Our finding that cyclic GMP formation was inhibited by NS 2028 in SIN-1-stimulated HUVEC and in NMDA-stimulated cerebellar slices and granule cells confirms the involvement of NO-regulated sGC in these responses, as revealed previously by use of ODQ (Garthwaite *et al.*, 1995). NS 2028 also largely inhibited vascular smooth muscle relaxations elicited by nitroglycerin and SNP, indicating that these relaxations were mediated by sGC. Furthermore, we recognized a specific inhibitory action of NS 2028 on NO-mediated relaxant responses of a non-vascular smooth muscle preparation from guinea-pig trachea. Thus, NS 2028 inhibited relaxations to nitroglycerin and electrical stimulation of i-NANC nerves, but not to unrelated cyclic AMP mediated relaxant pathways triggered by VIP, terbutaline and theophylline. Interestingly, while NS 2028 (1 $\mu$M) inhibited the NTG-elicited relaxations of histamine-contracted trachea by more than 75%, the i-NANC-mediated responses to electrical field stimulation were only inhibited by about 50%. This latter observation may be explained by the release of VIP, which has also been proposed to mediate i-NANC responses in the airways (Barnes, 1992).

The additional contraction induced by NS 2028 (0.1 – 1 $\mu$M) in isolated, endothelium-intact coronary arteries precon-stricted by $PGF_{2\alpha}$ indicates that the sGC in the arterial smooth muscle is constitutively activated by basally released endothelium-derived NO. In contrast, NS 2028 (0.03 – 1 $\mu$M) failed to enhance airway smooth muscle tone imposed by $PGF_{2\alpha}$ in guinea-pig trachea suggesting that the NO/guanylyl cyclase/cyclic GMP cascade is not constitutively activated in airway smooth muscle.

An apparently conflicting finding was that NS 2028 induced an irreversible inhibition of the isolated sGC, while the inhibition of NO-responsive sGC in coronary arteries was slowly reversible (50% recovery of SNP-induced relaxations after 2 h washout of NS 2028). However, a similar discrepancy has been observed with ODQ, which irreversibly inhibits bovine isolated lung sGC (Garthwaite *et al.*, 1995), but reversibly inhibits basal and NO-enhanced sGC activity in neuronal tissues *in vivo* (Fedele *et al.*, 1996). Several explanations may account for these observations: firstly, NS

2028- and ODQ-inhibited sGC could be reactivated by an unknown intracellular mechanism. Provided that oxidation of the haeme-iron underlies the inhibition of sGC by NS 2028 and its derivatives, the reactivating mechanism should facilitate reduction of ferric haeme GC to give the NO-responsive ferrous haeme enzyme. Alternatively, the oxidized haeme may be removed and ferrous haeme inserted into the apoenzyme. In favour of the latter hypothesis is the finding that haeme may move in and out of its sGC-pocket in the presence of lipophilic compounds (Foerster *et al.*, 1996), and that NO promotes haeme transfer from haemoproteins to apo-sGC (Ignarro *et al.*, 1986). A further possible mechanism to revert inhibition is the *de novo* synthesis of NO-responsive sGC. However, since the turnover of sGC protein and activity is slow (Shimouchi *et al.*, 1993; Liu *et al.*, 1997) the latter possibility seems unlikely.

In conclusion, we have demonstrated that NS 2028 is a potent and specific inhibitor of sGC in various biological systems including vascular and airway smooth muscle, endothelial cells, and cerebellum. Smooth muscle relaxant pathways triggered by the ANF-responsive particulate GC, adenylyl cyclase, and $K_{ATP}$-channels are not affected by this inhibitor. In intact cells inhibition was reversible, in contrast to the irreversible inhibition of the isolated sGC, suggesting the existence of yet unknown endogenous mechanisms to reactivate sGC. Oxidation and/or mobilization of the haeme-iron is a likely inhibitory mechanism, which could explain the irreversibility of inhibition *in vitro*. Variation of the substitu-tion at the benz-oxazine core structure influences the inhibitory potency of NS 2028-derivatives, suggesting specific interaction with a binding site (haeme-pocket?) on sGC. When working with these compounds one should be aware that they inhibit not only the NO-stimulated sGC activity, but also the basal, the YC-1 (Mülsch *et al.*, 1997) and the CO-enhanced activity (Mülsch, unpublished observations). Thus, NS 2028 and its derivatives are specific and potent tools to assess the involvement of sGC in biological responses and to differentiate sGC-dependent actions of NO, CO and NO-carriers from their sGC-independent actions.

## References

BARNES, P.J. (1992). Neural mechanisms in asthma. *Br. Med. Bull.*, **48**, 149 – 168.

BOHN, H. & SCHÖNAFINGER, K. (1989). Oxygen and oxidation promote the release of nitric oxide from sydnonimines. *J. Cardiovasc. Pharmacol.*, **14** (Suppl. 11), S6 – S12.

BRANDWEIN, H.J., LEWICKI, J.A. & MURAD, F. (1981). Reversible inactivation of guanylate cyclase by mixed disulfide formation. *J. Biol. Chem.*, **256**, 2958 – 2962.

BRÜNE, B. & SCHMIDT, K.U. & ULLRICH, V. (1990). Activation of soluble guanylate cyclase by carbon monoxide and inhibition by superoxide anion. *Eur. J. Biochem.*, **192**, 683 – 688.

BUSSE, R. & LAMONTAGNE, D. (1991). Endothelium-derived bradykinin is responsible for the increase in calcium produced by angiotensin-converting enzyme inhibitors in human endothe-lial cells. *Naunyn-Schmiedeberg's Arch. Pharmacol.*, **344**, 126 – 129.

DREJER, J., LARSSON, O.M. & SCHOUSBOE, A. (1983). Characteriza-tion of uptake and release processes for D- and L-aspartate in primary cultures of astrocytes and cerebellar granule cells. *Neurochem. Res.*, **8**, 231 – 243.

FEDELE, E., JIN, Y., VARNIER, G. & RAITERI, M. (1996). *In vivo* microdialysis study of a specific inhibitor of soluble guanylyl cyclase on the glutamate receptor nitric oxide cyclic GMP pathway. *Br. J. Pharmacol.*, **119**, 590 – 594.

FOERSTER, J., HARTENECK, C., MALKEWITZ, J., SCHULTZ, G. & KOESLING, D. (1996). A functional heme-binding site of soluble guanylyl cyclase requires intact N-termini of $\alpha_1$ and $\beta_1$ subunits. *Eur. J. Biochem.*, **240**, 380 – 386.

FÖRSTERMANN, U., ALHEID, U., FRÖLICH, J.C. & MÜLSCH, A. (1988). Mechanism of action of lipoxygenase and cytochrome P-450-mono-oxygenase inhibitors in blocking endothelium-depen-dent vasodilatation. *Br. J. Pharmacol.*, **93**, 569 – 578.

GARTHWAITE, J., SOUTHAM, E., BOULTON, C.L., NIELSEN, E.B., SCHMIDT, K. & MAYER, B. (1995). Potent and selective inhibition of nitric oxide-sensitive guanylyl cyclase by 1*H*-[1,2,4]oxadiazo-lo[4,3-$\alpha$]quinoxalin-1-one. *Mol. Pharmacol.*, **48**, 184 – 188.

GERZER, R., RADANY, E.W. & GARBERS, D.L. (1982). The separation of the heme and apoheme forms of soluble guanylate cyclase. *Biochem. Biophys. Res. Commun.*, **108**, 678 – 686.

GRYGLEWSKI, R.J., PALMER, R.M.J. & MONCADA, S. (1986). Superoxide anion is involved in breakdown of endothelium-derived vascular relaxing factor. *Nature*, **320**, 454 – 456.

IGNARRO, L.J., WOOD, K.S. & WOLIN, M.S. (1984). Regulation of purified soluble guanylate cyclase by porphyrins and metallo-porphyrins: A unifying concept. *Adv. Cycl. Nucl. Protein Phosphor. Res.*, **17**, 267 – 274.

IGNARRO, L.J., ADAMS, J.B., HORWITZ, P.M. & WOOD, K.S. (1986). Activation of soluble guanylate cyclase by NO-hemoproteins involves NO-heme exchange. *J. Biol. Chem.*, **261**, 4997 – 5002.

KIM, S., DEINUM, G., GARDNER, M.T., MARLETTA, M.A. & BABCOCK, G.T. (1996). Distal pocket polarity in the unusual binding site of soluble guanylate cyclase: Implications for the control of NO binding. *J. Am. Chem. Soc.*, **118**, 8769 – 8770.

KITZ, R. & WILSON, I.B. (1962). Esters of methanesulfonic acid as irreversible inhibitors of acetylcholinesterase. *J. Biol. Chem.*, **237**, 3245 – 3249.

LINCOLN, T.M. & CORNWELL, T.L. (1993). Intracellular cyclic GMP receptor proteins. *FASEB J.*, **7**, 328 – 338.

LIU, H., FORCE, T. & BLOCH, K.D. (1997). Nerve growth factor decreases soluble guanylate cyclase in rat pheochromocytoma PC12 cells. *J. Biol. Chem.*, **272**, 6038 – 6043.

LUOND, R.M., MCKIE, J.H. & DOUGLAS, K.T. (1993). A direct link between LY83583, a selective repressor of cyclic GMP formation, and glutathione metabolism. *Biochem. Pharmacol.*, **45**, 2547 – 2549.

MAYER, B., BRUNNER, F. & SCHMIDT, K. (1993). Inhibition of nitric oxide synthesis by methylene blue. *Biochem. Pharmacol.*, **45**, 367 – 374.

MÜLSCH, A. & BÖHME, E. (1984). UV/VIS- and EPR-spectroscopic investigation of soluble guanylate cyclase. Activation by NO and sydnonimines. *Naunyn-Schmiedeberg's Arch. Pharmacol.*, **325**, R31.

MÜLSCH, A., BUSSE, R., LIEBAU, S. & FÖRSTERMANN, U. (1988). LY 83583 interferes with the release of endothelium-derived relaxing factor and inhibits soluble guanylate cyclase. *J. Pharmacol. Exp. Ther.*, **247**, 283 – 288.

MÜLSCH, A. & BUSSE, R. (1990). $N^G$-nitro-L-arginine (N5-[imino(nitroamino)methyl-L-ornithine) impairs endothelium-dependent dilations by inhibiting cytosolic nitric oxide synthesis from L-arginine. *Naunyn-Schmiedeberg's Arch. Pharmacol.*, **341**, 143 – 147.

MÜLSCH, A., BAUERSACHS, J., SCHÄFER, A., STASCH, J.-P., KAST, R. & BUSSE, R. (1997). Effect of YC-1, an NO-independent, superoxide-sensitive stimulator of soluble guanylyl cyclase, on smooth muscle responsiveness to nitrovasodilators. *Br. J. Pharmacol.*, **120**, 681 – 689.

MÜLSCH, A. & GERZER, R. (1991). Purification of heme-containing soluble guanylyl cyclase. In *Methods Enzymol*. Vol. 195: *Adenyl cyclase, G Proteins, and Guanylyl Cyclase*. ed. Johnson, J.A. & Corbin, J.D. pp.377 – 383. San Diego: Academic Press.

NG, D.D.W. & DIAMOND, J. (1986). Effects of LY83583 on atriopeptin II induced relaxations and cyclic GMP elevation in the rabbit aortic rings. *Proc. West. Pharmacol. Soc.*, **29**, 113 – 116.

NIELSEN-KUDSK, F., POULSEN, B., RYOM, C. & NIELSEN-KUDSK, J.E. (1986). A strain-gauge myograph for isometric measurements of tension in isolated small blood vessels and other muscle preparations. *J. Pharmacol. Methods*, **16**, 215 – 225.

O'DONNEL, M.E. & OWEN, N.E. (1986). Role of cyclic GMP in atrial natriuretic factor stimulation of $Na^+$, $K^+$, $Cl^-$ cotransport in vascular smooth muscle cells. *J. Biol. Chem.*, **261**, 15461 – 15466.

OHLSTEIN, E.H., WOOD, K.S. & IGNARRO, L.J. (1982). Purification and properties of heme-deficient hepatic soluble guanylyl cyclase: Effects of heme and other factors on enzyme activation by NO, NO-heme, and protoporphyrin IX. *Arch. Biochem. Biophys.*, **218**, 187 – 198.

SCHMIDT, H.H.H.W., LOHMANN, S.M. & WALTER, U. (1993). The nitric oxide and cGMP signal transduction system: Regulation and mechanisms of action. *Biochem. Biophys. Acta*, **1178**, 153 – 175.

SCHRAMMEL, A., BEHRENDS, S., SCHMIDT, K., KOESLING, D. & MAYER, B. (1996). Characterization of 1*H*-[1,2,4]oxadiazolo[4,3-a]quinoxalin-1-one as a heme-site inhibitor of nitric oxide-sensitive guanylyl cyclase. *Mol. Pharmacol.*, **50**, 1 – 5.

SHIMOUCHI, A., JANSSENS, S.P., BLOCH, D.B., ZAPOL, W.M. & BLOCK, D.B. (1993). cAMP regulates soluble guanylate cyclase $\beta$1-subunit gene expression in RFL-6 rat fetal lung fibroblasts. *Am. J. Physiol.*, **265**, L456 – L461.

STONE, J.R. & MARLETTA, M.A. (1995). The ferrous heme of soluble guanylate cyclase: Formation of hexacoordinate complexes with carbon monoxide and nitrosomethane. *Biochemistry*, **34**, 16397 – 16403.

STONE, J.R., SANDS, R.H., DUNHAM, W.R. & MARLETTA, M.A. (1996). Spectral and ligand-binding properties of an unusual hemoprotein, the ferric form of soluble guanylate cyclase. *Biochemistry*, **35**, 3258 – 3262.

WEDEL, B., HUMBERT, P., HARTENECK, C., FOERSTER, J., MAL-KEWITZ, J., BÖHME, E., SCHULTZ, G. & KOESLING, D. (1994). Mutation of His-105 in the $\beta_1$ subunit yields a nitric-oxide-insensitive form of soluble guanylyl cyclase. *Proc. Natl. Acad. Sci. U.S.A.*, **91**, 2592 – 2596.